Preprints of the 21st IFAC World Congress (Virtual)
Berlin, Germany, July 12-17, 2020

Ex-post Analysis of the WEC Control Competition Results Using a Fourier Spectral Control Approach

Alexis Mérigaud * **Caroline Ngo** * **Hoai-Nam Nguyen** **
Guillaume Sabiron ** **Paolino Tona** **

* *IFP Energies Nouvelles - établissement de Rueil, 1 et 4 avenue de Bois-Préau, 92852 Rueil-Malmaison, France (contact e-mail: alexis.merigaud@ifpen.fr).*
** *IFP Energies Nouvelles - établissement de Lyon, Rond-point de l'échangeur de Solaize, 69360 Solaize, France (contact e-mail: paolino.tona@ifpen.fr).*

Abstract: The wave energy converter control competition (WECCCOMP) allowed several real-time control approaches to be assessed, both in numerical and physical experiments. The solution retained by IFP Énergies Nouvelles (IFPEN), which won the numerical simulation and experimental evaluation phases, consists of a receding-horizon MPC algorithm, including an estimator and a predictor for the wave excitation torque. The control objective function, solved by a quadratic programming (QP) optimiser in the real-time implementation, is weighted over the receding time horizon by means of weighting coefficients, which are optimised off-line for each sea state, in order to take into account the non-ideal power take-off (PTO) efficiency. Given the potential complexity of the interaction between the different components involved in the control implementation (estimation, prediction, QP solution, choice of weightings), it is useful to carry out an ex-post analysis, in order to understand if, and how, the solution proposed by IFPEN could have been improved. To that end, a Fourier spectral control algorithm is implemented, which is able to calculate the optimal trajectory and control torque for the totality of a signal, simulated from WECCCOMP sea states, taking the non-ideal PTO efficiency into account. By comparing MPC results with the theoretically optimal solutions provided by the spectral method, it is found that, in the studied WECCCOMP sea states, the IFPEN MPC algorithm performance lies within approximately 10% of the optimal solution, in terms of electric power. The influence of the MPC forecast accuracy and prediction horizon is examined. Finally, some challenges associated with the offline MPC weighting optimisation are identified.

Keywords: Wave energy converters, Power-maximising control, Model predictive control, Spectral control, Non-smooth optimal control

1. INTRODUCTION

Real-time power-maximising control is seen as a promising path towards cheaper wave energy harvesting, see for example Ringwood et al. (2014). A large variety of wave energy converter (WEC) control algorithms have thus been investigated, from relatively simple parametric controllers to more sophisticated model predictive control (MPC) algorithms, as reviewed by Faedo et al. (2017). However, comparison between existing control approaches is difficult, because published works, regarding different control strategies, also typically differ with respect to the WEC models and sea states considered. Furthermore, few studies exist reporting the implementation of control strategies in physical experiments. Announced in 2017 by Ringwood et al. (2017), the WEC control competition (WECCCOMP) provided a framework for a fair comparison between different algorithms, including physical experiments on a scale WEC model in a wave tank.

The objective of WECCCOMP contestants consisted in designing a real-time power-maximising control algorithm for a scale model of the Wavestar device [1], evaluated in both numerical and physical experiments, corresponding to the two phases of the competition:

- In the numerical simulation phase, the competing solutions were assessed in a WECSIM [2] simulation environment, in wave excitation signals generated from six different sea states.
- Experimental tests took place in Aalborg University (Denmark) in May 2019, consisting of 3 realisations for each of the six sea states of the competition.

In addition to the requirements usually associated with WEC control, such as wave excitation estimation and prediction, the WECCCOMP control evaluation framework presents several specific challenges from a control implementation perspective. Firstly, the small scale of the

[1] http://wavestarenergy.com/
[2] https://wec-sim.github.io/WEC-Sim/

device, and the corresponding short wave periods of the competition sea states, imply shorter control time steps than in a full-scale implementation, thus making the real-time compatibility of the proposed algorithms more challenging. Furthermore, the WECCCOMP model includes an electrical power take-off (PTO) system with a non-ideal efficiency function, which results in a non-quadratic, non-convex objective function with discontinuous derivatives, to be optimised by the control algorithm at each control update.

The control solution proposed by IFP Energies Nouvelles (IFPEN), which is a receding-horizon MPC scheme detailed by Tona et al. (2019), came first in the two phases of the competition. However, this success only constitutes a relative result, as it does not indicate how far all competitors were from the actual optimal power, which could have been achieved by the WECCCOMP model in the same sea states, under optimal control.

In this paper, a spectral method, derived from Mérigaud and Ringwood (2017), is employed to compute the optimal control torque, trajectory and mean electrical power, for the WECCCOMP model in random realisations of the competition sea states. Such results assume that the totality of the wave excitation signal is known and are not limited by the requirements of real-time compatibility; they therefore constitute an upper bound to the performance of any control algorithm working in a real-time, receding-horizon configuration.

An ex-post analysis of IFPEN's MPC algorithm is carried out in two steps. Firstly, the MPC algorithm is compared with the spectral control method in identical realisations, representative of the WECCCOMP sea states. This allows for assessing the performance of IFPEN's algorithm in absolute terms, through comparison with an optimal control solution. Then, various hypothesis are investigated in order to explain the differences observed between the MPC performance and optimal control results, and to find paths of improvement.

In the present study, in order to facilitate the interpretation of control results, the following simplifications are made with respect to the two WECCCOMP phases:

- The PTO internal dynamics are not considered, as those had been found to have very minor effects upon the controller's performance in the numerical evaluation framework, and were not emulated in the experimental evaluation phase.
- The hydromechanical model used to optimise and assess the controllers is linear (unlike the numerical model implemented in the WECSIM environment, which includes mechanical non-linearities); therefore the controllers are evaluated in simulations based on the nominal WEC model.
- Only the average electric power is optimised, as opposed to the WECCCOMP evaluation criterion, that also penalises large position, control input and power excursions.

The rest of this paper is organised as follows:

- In Section 2, the mathematical model of the WECCCOMP device is introduced, and the control problem is formulated.
- Section 3 presents the MPC solution retained by IFPEN.
- Section 4 details the offline spectral control method employed in this study.
- The numerical experiments and their results are described and commented in Section 5.
- Conclusions are presented in Section 6.

2. THE WECCCOMP CONTROL PROBLEM

2.1 WEC dynamical model

In the present study, the Wavestar mathematical model is linearised around the mean angular position of the rotational arm [3] . The model expresses the balance between torques calculated at the rotation point. It is identical to that, identified by the competition organisers and documented by Ringwood et al. (2017), and takes the form of the well-known Cummins equation:

$$(I + I_\infty)\ddot{x} + c_v\dot{x} + k_\mathrm{r} \circledast \dot{x} + Kx = e + u \qquad (1)$$

of which the terms can be thus detailed:

- x is the angular position deviation.
- I is the rotational inertia of the float and its arm in the rotation point.
- The moment, in the rotation point, of radiation forces, is expressed as the sum of inertial terms $I_\infty\ddot{x}$, and memory effects, $k_\mathrm{r} \circledast \dot{x} = \int_0^t k_\mathrm{r}(\tau)\dot{x}(t-\tau)d\tau$, where $k_\mathrm{r}(\tau)$ is the convolution kernel corresponding to radiation forces in the rotation point. However, in the WECCCOMP model, the convolution term is approximated by means of a state-space model of order 2, see Ringwood et al. (2017).
- $c_v\dot{x}$ represents a damping term, which aims at taking into account friction, both in the fluid and at the arm joint.
- Kx represents the hydrostatic stiffness moment.
- e is the moment of the excitation wave torque exerted onto the floater by incident waves.
- u is the moment of the force applied by the linear generator. u is the control variable which has to be optimised.

The dynamical equations can also be expressed in the frequency domain in the following manner:

$$z(\omega)\hat{x}(\omega) = \hat{e}(\omega) + \hat{u}(\omega) \qquad (2)$$

where $z(\omega) = K - \omega^2(I + a_\mathrm{r}(\omega)) - j\omega(c_v + b_\mathrm{r}(\omega))$, and a_r and b_r are frequency-dependent added-mass and damping terms, respectively, which are related to I_∞ and k_r through formula given by Ogilvie (1964).

[3] Note that, in the first WECCCOMP phase, the simulation framework included some non-linear effect in the mechanical arm rotation and torque calculations. In contrast, in the present study, the linear model is employed both by the controller and in the numerical simulations, which avoids modelling inconsistencies between linear hydrodynamics and non-linear rotational motion representation, and considerably simplifies the analysis.

2.2 Optimal control problem formulation

In the WECCCOMP case study, the non-ideal PTO system is modelled by means of a non-unity efficiency factor $\mu = 0.7$ so that, denoting the instantaneous absorbed hydromechanical power as $p_a(\dot{x}, u) = -u(t)\dot{x}(t)$, the instantaneous electric power is expressed as follows:

$$p_e(\dot{x}, u) = \begin{cases} \mu p_a(\dot{x}, u) & \text{if } p_a(\dot{x}, u) \geq 0 \\ \dfrac{1}{\mu} p_a(\dot{x}, u) & \text{if } p_a(\dot{x}, u) \leq 0 \end{cases} \tag{3}$$

Define $h(p_a)$ the efficiency function, equal to μ for positive p_a, and $1/\mu$ for negative p_a. Such a discontinuous function is undesirable from a control implementation perspective, for both spectral and MPC approaches. How this discontinuous efficiency function is dealt with, within the MPC and spectral control frameworks, will be specified in corresponding Sections 3 and 4.

Define $\mathcal{L}\{x\} := (I+I_\infty)\ddot{x} + c_v\dot{x} + k_\mathrm{r} \circledast \dot{x} + Kx$. The optimal control problem takes the following form:

$$\begin{cases} \max f(x, u) = \dfrac{1}{T_h} \displaystyle\int_{t=0}^{T_h} p_e(\dot{x}, u) dt \\ \text{s.t. } \mathcal{L}\{x\} = u(t) + e(t) \end{cases} \tag{4}$$

where T_h is the control time horizon, and the equality constraint expresses the fact that the dynamical equation (1) must be satisfied at every instant. Finally, like in IFPEN's WECCCOMP solution, an additional constraint is added onto the control input magnitude, in the form $|u| \leq u_{\max}$, where $u_{\max} = 10$ N.m.

3. THE IFPEN MPC SOLUTION

The main advantage of MPC, as applied to WEC control, is the ability to solve the power maximising control problem in a receding-horizon configuration, using wave excitation moment predictions, based on a discrete-time model of the WEC dynamics. MPC is also well known for efficiently coping with actuator and state constraints. At each time step of an MPC algorithm, the optimal control problem is solved over the receding time horizon. The resulting control input is only applied at the current time step and, at the next time step, the optimal control problem is solved again, with updated variables.

IFPEN's real-time MPC strategy, an overview of which is given by Nguyen et al. (2016), was tested on a Wavestar scale model in the Aalborg University wave basin in 2015, and again in 2019 for the WECCCOMP. It comprises the three main components shown in Fig. 1: wave excitation moment estimation, short-term wave excitation moment prediction, and online control problem solution. A brief description of each component is given in the following subsections. For further details on the MPC scheme, the reader should refer to the article by Nguyen et al. (2016) and other works by the same authors.

3.1 WEC dynamical model for control

From Eq.(1), a linear state-space model is derived. The resulting design model is a 4^{th}-order linear state-space representation and is expressed as follows:

$$\begin{aligned} A_c &= \begin{bmatrix} 0 & 1 & \mathbf{0}_{1\times 2} \\ -\dfrac{K}{I+I_\infty} & -\dfrac{D_\mathrm{r}+c_v}{I+I_\infty} & -\dfrac{C_\mathrm{r}}{I+I_\infty} \\ 0 & B_\mathrm{r} & A_\mathrm{r} \end{bmatrix}, \\ B_c &= \begin{bmatrix} 0 \\ \dfrac{1}{I+I_\infty} \\ \mathbf{0}_{2\times 1} \end{bmatrix}, \quad C_c = \begin{bmatrix} 1 & 0 & \mathbf{0}_{1\times 2} \\ 0 & 1 & \mathbf{0}_{1\times 2} \end{bmatrix} \end{aligned} \tag{5}$$

where $\mathbf{0}_{i\times j}$ is a i-row and j-column zero matrix and A_r, B_r, C_r, D_r are the state-space representation matrices of the 2^{nd} order radiation model, with entries provided by the organisers, see Ringwood et al. (2017). In the following, $\mathbf{X} = (x, \dot{x}, x_\mathrm{r})^T$ denotes the state variables, with x_r the state vector of radiation state-space model, $U = e + u$ denotes the input variable and $\mathbf{Y} = (x, \dot{x})^T$, the output variables.

IFPEN's MPC solution requires a discretisation of the WEC dynamics and control problem. The WEC dynamics are discretised using bilinear Tustin's method to obtain matrices A_d, B_d and C_d from A_c, B_c and C_c.

3.2 Wave excitation moment estimation and prediction

The wave excitation moment is not directly available to measurement during WEC operation, and hence must be estimated from the WEC dynamics. To achieve this, a linear Kalman filter (LKF), whereby the wave excitation randomness is represented by means of a random walk model, is used to estimate the state X, based on the model described by (5). The time series, obtained with present and past estimated values of excitation moments, is employed by an adaptive bank of Kalman filters (AKF) to compute the prediction over a short time horizon. The AKF method is designed to automatically adapt autoregressive (AR) coefficients to the current sea state. Both LKF and AKF run with a sample time of 50 ms. An AR model of order 16 and a prediction horizon of $N_p = 25$ samples (1.25 s) were used during the WECCCOMP.

The chosen estimation and prediction approaches are dealt with more specifically by Nguyen and Tona (2018). Note that, in the current study, no model mismatch exists between the nominal and actual WEC models; furthermore, no measurement noise is simulated. This certainly simplifies the task of the wave excitation estimator, although the latter demonstrated accurate performance in the 2019 physical experiments.

3.3 MPC optimal control formulation

Once the wave excitation moment prediction is obtained, the optimal control is computed over the prediction hori-

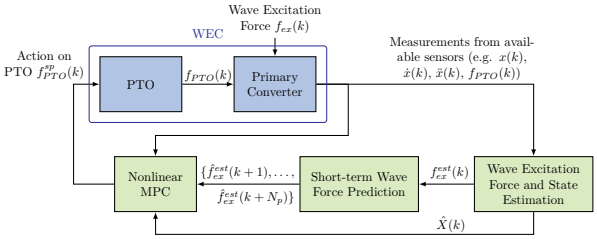

Fig. 1. IFPEN's MPC scheme

zon to maximise the average electrical power, taking into account the PTO efficiency h.

The discrete-time optimal control problem, over the prediction horizon of N_p time steps, can be formulated as follows, using the second-order Runge-Kutta method (trapezoidal rule) for accurate discretisation:

$$\max_{u(k|k),\dots,u(k+N_p-2|k)} \sum_{j=0}^{N_p-2} \mathcal{P}_e(k+j|k)$$
$$\text{s.t.} \begin{cases} X(k+j+1|k) = A_d X(k+j|k) + B_d \tilde{U}(k+j|k) \\ -u_{\max} \leq u \leq u_{\max} \end{cases} \tag{6}$$

where:

- The discretised electric power is expressed as $\mathcal{P}_e(k+j|k) = h(k+j|k)u(k+j|k)[\dot{x}(k+j|k)+\dot{x}(k+j+1|k)]$.
- $X(k+j|k)$ and $\tilde{U}(k+j|k) := u(k+j|k) + \tilde{e}(k+j|k)$ denote, respectively, the predicted state and input variables at time $k+j$ from time step k, where $\tilde{e}(k+j|k)$ is the wave excitation moment predicted from the AKF.
- $h(k+j|k)$ and $\dot{x}(k+j|k)$ denote, respectively, the predicted PTO efficiency and angular velocity at time $k+j$ from time step k.

3.4 Dealing with a non-ideal efficiency function

Solving (6) is computationally challenging, as h is a nonlinear, discontinuous function. The discontinuity could be addressed by approximating h with a smooth function, but the convexity of the resulting optimisation problem would still not be guaranteed. To deal with non-convexity, a new discrete objective function is introduced, with *fixed* coefficients q_j which replace $h(k+j|k)$ in (6), thus weighting the instantaneous mechanical power values over the prediction horizon. The weightings $q_j \geq 0$ then become tuning parameters for a new optimisation problem, which is a convex quadratic programming (QP) problem.

Those weightings, which form the key aspect of the proposed MPC optimisation scheme, are optimised off-line on a sea-state by sea-state basis, in order to ensure that optimising the new objective function also optimises, as much as possible, the original objective function in (6). An offline procedure, based on repeated simulations of the MPC scheme, is used to obtain the set of weightings which maximises average electric power, for a given sea state or for a combination of sea states. A gradient-free optimisation method is required to cope with the singularity and non-convexity of the underlying objective function. The Nelder-Mead simplex (NMS) method, which is computationally compact and converges for a large class of problems, see **?**, was chosen.

Thus, all in all, this approach shifts the complexity of optimising the original objective function online to an offline optimisation procedure, which is not subject to real-time computational constraints. Once the optimal weightings are found, running the MPC algorithm reduces to solving a convex QP problem, which can be efficiently done online. During the WECCCOMP experimental evaluation, for instance, the whole MPC system was able to run in less than 1 ms, well below the control time step of 50 ms.

Note that the weightings do not necessarily have a physical interpretation. For instance, the magnitude of the optimal weightings could be expected to be decreasing over the prediction horizon, in order to penalise those time instants, where predictions are less accurate. However, in general, the weightings chosen by the offline optimisation procedure do not exhibit any particular trend.

4. FOURIER SPECTRAL CONTROL APPROACH

4.1 Spectral optimal control formulation

The spectral control calculation approach, employed in the present study, is an extension of that introduced by Mérigaud and Ringwood (2017), to the case of a more general objective function of the form $\alpha(x, \dot{x}, u)$.

At this stage, it must be made clear that the spectral method, as employed in this work, is not implemented in a receding-horizon fashion. Instead, the totality of a simulated wave signal ($T_{sim} = 40$s, typically covering between 20 and 40 wave periods) is considered, and the spectral method is used to calculate the optimal control solution over the whole wave signal *at once*. This provides the performance which could be achieved, by a controller having a perfect knowledge of wave excitation moments for an arbitrarily long time into the future. Therefore, while, in the MPC configuration, the period T_h of Eq. (4) corresponds to that of the receding horizon, in the context of spectral control $T_h = T_{sim}$ represents the totality of the wave signal duration.

Given the particular form of the dynamical equation (1), u can be expressed as a function of the other variables, so that Problem (4) can be recast as follows:

$$\max f(x) = \frac{1}{T_{sim}} \int_{t=0}^{T_{sim}} p_e(\dot{x}, \mathcal{L}\{x\} - e)dt \tag{7}$$

where the variable u and the equality constraints are eliminated, so that only the device trajectory is now optimised.

Assume a periodic, polychromatic excitation signal with period T_{sim}, of the form

$$e(t) = \frac{1}{\sqrt{2}}\hat{e}_1 + \sum_{n=1}^{N} \hat{e}_{2n}\cos(\omega_n t) + \hat{e}_{2n+1}\sin(\omega_n t) \tag{8}$$

where the frequencies ω_n are defined harmonically with $\Delta\omega = \frac{2\pi}{T_{sim}}$ and $\forall n \in \{1...N\}, \omega_n = n\Delta\omega$, with N corresponding to the cutoff harmonic. In the following, consistently with a periodic excitation signal, solutions x are searched amongst periodic signals with period T_{sim} so that, in essence, only steady-state solutions to the control problem are considered. The WEC motion is also assumed of the form:

$$x(t) = \frac{1}{\sqrt{2}}\hat{x}_1 + \sum_{n=1}^{N} \hat{x}_{2n}\cos(\omega_n t) + \hat{x}_{2n+1}\sin(\omega_n t) \tag{9}$$

The next step consists in discretising the integral objective function, using a set of M equally-spaced points t_m, spanning the interval $[0; T_{sim}]$, with typically $M \geq 2N+1$, so that the maximisation problem becomes:

$$\max \tilde{f}(x) := \sum_{m=1}^{M} p_e(t_m) \tag{10}$$

where, for the sake of conciseness, $p_e(t_m)$ denotes the value of p_e when its arguments are evaluated at time instants t_m.

Define the matrix $\Phi \in \mathbb{R}^{M\times(2N+1)}$ as:

$$\forall i \in \{1...M\}, j \in \{1...N\}, \begin{cases} \Phi_{i,1} = 1/\sqrt{2} \\ \Phi_{i,2j} = \cos(\omega_j t_i) \\ \Phi_{i,2j+1} = \sin(\omega_j t_i) \end{cases} \quad (11)$$

and the matrix

$$\Omega = \begin{pmatrix} \Omega_0 & \cdots & 0 \\ \vdots & \ddots & \vdots \\ 0 & \cdots & \Omega_N \end{pmatrix} \quad (12)$$

where $\Omega_0 = 0$ and, $\forall n \geq 1$, $\Omega_n = \begin{pmatrix} 0 & \omega_n \\ -\omega_n & 0 \end{pmatrix}$.

Define vectors $\hat{\mathbf{x}} := (\hat{x}_1 \cdots \hat{x}_N)^\intercal$, $\hat{\mathbf{e}} := (\hat{e}_1 \cdots \hat{e}_N)^\intercal$, $\mathbf{x} := (x(t_1) \cdots x(t_M))^\intercal$, $\dot{\mathbf{x}} := (\dot{x}(t_1) \cdots \dot{x}(t_M))^\intercal$ and $\mathbf{e} := (e(t_1) \cdots e(t_M))^\intercal$. Then, it is easy to see that $\mathbf{x} = \Phi\hat{\mathbf{x}}$, $\dot{\mathbf{x}} = \Phi\Omega\hat{\mathbf{x}}$ and $\mathbf{e} = \Phi\hat{\mathbf{e}}$.

Furthermore, the terms of $\mathcal{L}$ evaluated at times $t_1...t_M$, $l := (\mathcal{L}\{x\}(t_1) \cdots \mathcal{L}\{x\}(t_M))^\intercal$, can be calculated as $l = \Phi\mathbf{L}\hat{\mathbf{x}}$, where

$$\mathbf{L} = \begin{pmatrix} L_0 & \cdots & 0 \\ \vdots & \ddots & \vdots \\ 0 & \cdots & L_N \end{pmatrix} \quad (13)$$

with blocks $L_0 = \Re\{z(0)\}$ and $\forall n \in \{1...N\}$, $L_n = \begin{pmatrix} \Re\{z(\omega_n)\} & \Im\{z(\omega_n)\} \\ -\Im\{z(\omega_n)\} & \Re\{z(\omega_n)\} \end{pmatrix}$.

Finally, the objective function can be expressed as a function of $\hat{\mathbf{x}}$, as follows:

$$\tilde{f}(\hat{\mathbf{x}}) = \mathbf{1}_{M\times 1}^\intercal \mathbf{p_e}(\Phi\Omega\hat{\mathbf{x}}, \Phi\mathbf{L}\hat{\mathbf{x}} - \Phi\hat{\mathbf{e}}) \quad (14)$$

where $\mathbf{1}_{M\times 1}$ is the unit vector of size $M\times 1$, and $\mathbf{p_e}$ denotes the vector obtained when p_e is applied component-wise to the arguments, i.e. for example, $\mathbf{p_e}(\mathbf{v}) = (p_e(\mathbf{v}_1)...p_e(\mathbf{v}_M))^\intercal$.

The first- and second-order derivatives of $\tilde{f}$, with respect to the components of $\hat{\mathbf{x}}$, can be calculated explicitly; however, for the sake of conciseness, the mathematical details are not reproduced here. Those derivatives are used within a gradient-based optimisation algorithm, to ensure a fast convergence to the solution.

4.2 Dealing with a non-ideal efficiency function

The non-ideal efficiency function is undesirable for the proposed spectral control implementation, which employs 1st- and 2nd-order derivatives of the objective function. Therefore, for the spectral control calculations carried out in this study, the efficiency function $p_e = h(p_a)$ is approximated by means of the following function:

$$\tilde{h}_\kappa(p_a) = A\tanh(\kappa p_a) + B \quad (15)$$

where $A = \frac{1}{2}(\mu - 1/\mu)$, $B = \frac{1}{2}(\mu + 1\mu)$, and $\kappa > 0$ is a real parameter, which governs the accuracy of the approximation, as illustrated in Fig. 2.

For all $(\dot{x}, u)$, $p_e(\dot{x}, u) \leq p_{e,\kappa}(\dot{x}, u)$. Therefore, the optimal mean electric power, $\overline{P}^*_{e,\kappa}$, obtained with $p_{e,\kappa}$, is an upper bound to the optimal exact electric power, $\overline{P}^*_e$, which would be obtained if Problem (10) could be solved using the exact efficiency. Furthermore, for all $\kappa_1 \leq \kappa_2$, for all $(\dot{x}, u)$, $p_{e,\kappa_2}(\dot{x}, u) \leq p_{e,\kappa_1}(\dot{x}, u)$, which implies that $\overline{P}^*_{e,\kappa}$ decreases monotonically with κ, and has $\overline{P}^*_e$ as a limit when $\kappa \to \infty$.

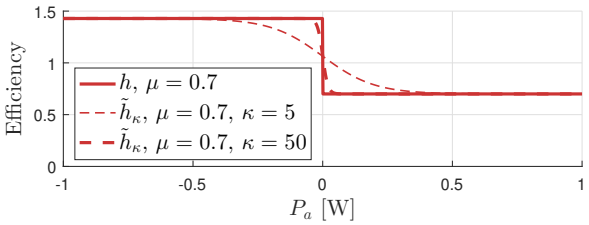

Fig. 2. Efficiency function h and its approximations $\tilde{h}_\kappa$

$\overline{P}^*_e$ can also be bounded from below: consider the solution x^*_κ, u^*_κ, obtained with the approximate objective function. x^*_κ, u^*_κ is necessarily sub-optimal, with respect to the exact objective function. Therefore, the exact mean electric power, effectively achieved with (x^*_κ, u^*_κ), constitutes a lower bound to $\overline{P}^*_e$, and is calculated as follows:

$$\overline{P}^\dagger_{e,\kappa} = \frac{1}{T_{sim}} \int_{t=0}^{T_{sim}} p_e(\dot{x}^*_\kappa, u^*_\kappa) dt \quad (16)$$

Therefore the following inequality holds:

$$\overline{P}^\dagger_{e,\kappa} \leq \overline{P}^*_e \leq \overline{P}^*_{e,\kappa} \quad (17)$$

Even if the true optimal electrical power $\overline{P}^*_e$ cannot be calculated for the exact efficiency, by setting κ to a large enough value, it can be ensured that the electric power $\overline{P}^\dagger_{e,\kappa}$, effectively achieved with the solution found, lies within a prescribed percentage of $\overline{P}^*_e$.

Throughout the rest of this paper, mean electric power values, obtained from the spectral control method, are in fact $\overline{P}^\dagger_{e,\kappa}$, for κ chosen sufficiently large so that $\overline{P}^\dagger_{e,\kappa}$ lies well within 2% of $\overline{P}^*_e$.

5. NUMERICAL RESULTS

5.1 Numerical set-up

MPC and spectral control methods are assessed in 40s wave signals, randomly generated from WECCCOMP sea states 1 (JONSWAP with $\gamma = 1$, $H_{m_0} = 0.0208$m and $T_p = 0.988$s) and 3 (JONSWAP with $\gamma = 1$, $H_{m_0} = 0.1042$m and $T_p = 1.836$s), abbreviated as SS1 and SS3. Although longer signals would provide better statistical accuracy, 40s cover between 20 and 40 typical wave periods, and were found sufficient for relative performance assessment of spectral and MPC approaches, while permitting efficient spectral control calculations, and easing the offline MPC weighting optimisation. Three 40s random realisations (R1, R2, R3) are generated for each sea state, using a summation of sinusoids with independent, uniformly distributed random phases, and amplitudes derived from the wave spectrum.

Spectral control solutions are calculated in every random realisation, taking into account PTO constraints, using the interior point optimisation algorithm, readily implemented in the Matlab [4] *fmincon* function.

[4] www.matworks.com

	SS1 ($.10^{-2}$)			SS3		
	R1	R2	R3	**R1**	R2	R3
Spectral - $\mu = 1$	**3.14**	3.14	3.14	**1.31**	1.32	1.25
Spectral - $\mu = 0.7$	**2.14**	2.11	2.13	**0.79**	0.80	0.75
WECCCOMP MPC	**1.96**	1.93	1.93	**0.71**	0.72	0.66
MPC (perfect pred.)	**2.01**	1.95	1.96	**0.71**	0.74	0.68
Passive control	**1.64**	1.64	1.64	**0.37**	0.37	0.37

Table 1. Mean electrical power [W] from MPC and spectral solutions

For both sea states, MPC weightings are optimised offline using realisation R1, and the strategy is then evaluated in R1, R2 and R3. As mentioned in the introduction, in a first step, the MPC implementation parameters are set as close as possible to the WECCCOMP conditions: the receding horizon length is set to $N_p = 25$ (1.25 s), and the offline optimisation is initialised with all weightings equal to 1. Wave excitation prediction is carried out using the AKF. More information regarding the chosen baseline settings may be found in Tona et al. (2020).

Subsequently, various paths are investigated, to explain and reduce the difference between MPC and spectral control results. In particular, excitation estimations and predictions are replaced with their exact values, and the influence of the receding horizon length N_p is examined. Furthermore, several initialisation methods are tested for the offline weighting optimisation algorithm, with the hope of converging to better weightings.

5.2 Comparison of MPC and spectral control results

Table 1 compares WECCCOMP MPC and spectral control results, in SS1 and SS3. A look at the 2nd and 3rd rows indicates that, for both sea states, the WECCCOMP MPC solution lies reasonably close to the optimal electrical power, calculated through the spectral method: approx. 8.5% for SS1, R1, and 10.5% for SS3, R1. The difference further reduces to approximately 6% for SS1, R1, and 9.5% for SS3, R1, when perfect excitation predictions are assumed (row 4 of Table 1). In addition, it is found that, although MPC weightings are optimised solely based on R1, the MPC performance, relative to optimal control, is consistent across the three realisations, which demonstrates the robustness of the proposed MPC scheme to the random realisation employed for the offline optimisation phase.

Additional points of comparison are provided by Table 1. In the two WECCCOMP sea states, the optimal electric power, achievable with $\mu = 0.7$, is approximately 60% of the ideal case with $\mu = 1$, shown in the 1st row. Furthermore, wave periods in SS1 are relatively close to the WEC resonant period; therefore, the benefit of employing active control strategies (spectral and MPC), with respect to a simple linear damping constant (last row of Table 1), is relatively small. In contrast, SS3 is further away from the WEC resonant frequency, and therefore makes active control strategies highly beneficial, with a twofold increase in mean electrical power with respect to the simple damping constant.

MPC and optimal control results may also be compared in terms of control solutions, which is done in Fig. 3 for SS1, R1, and Fig. 4 for SS3, R1. However, before examining

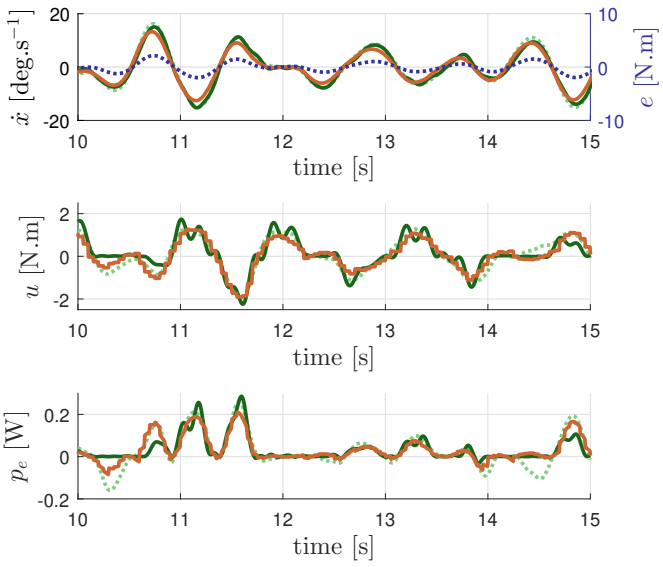

Fig. 3. Control solutions in sea state 1, in terms of velocity, control input and electrical power, obtained with the spectral method for $\mu = 1$ (dotted green), and for $\mu = 0.7$ with the spectral (green) and MPC (orange) methods. Also shown on the first graph, the wave excitation torque (dotted blue).

the MPC solution, it is useful to first elaborate on optimal control results obtained through the spectral method, with a perfect PTO efficiency *vs* with $\mu = 0.7$.

In SS1, with an ideal PTO, some reactive power (negative values in the 3rd graph of Fig. 3) is employed to achieve optimal power absorption. In contrast, when a non-ideal PTO efficiency is considered, the optimal solution, obtained through the spectral method, ensures that very little reactive power is used. This is achieved through significant modifications in the control input (see the differences between the solid and dotted green curves, in the second graph of Fig. 3).

In SS3, which has waves with periods further away from the WEC resonant frequency, large amounts of reactive power are employed to achieve optimal control, when $\mu = 1$ (dotted green line in the last graph of Fig. 4). This greatly amplifies the contrast with the non-ideal PTO case, for which optimal control requires the suppression of the vast majority of reactive power. Consequently, differences between the optimal solutions with ideal *vs* non-ideal PTO are strongly marked, both in terms of velocity trajectory (1st graph) and control input (2nd graph).

In both sea states, the WECCCOMP MPC scheme shows velocity trajectories and control inputs which are relatively close to the optimal ones, as can be appreciated by comparing solid green and orange curves in Figs. 3 and 4. It can be observed, from the 3rd graph in Figs. 3 and 4, that the proposed MPC scheme succeeds in employing relatively little reactive power, although less drastically than the optimal control solution. Indeed, the MPC weightings can only be optimised so as to take the non-ideal PTO efficiency into account *on average*, for a given sea state.

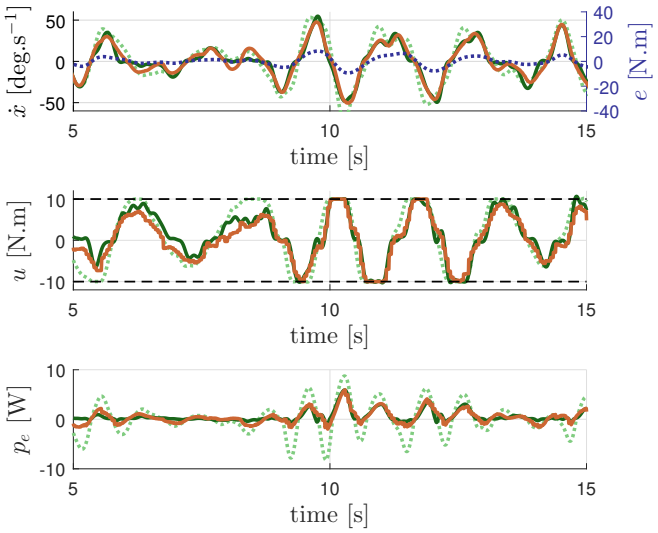

Fig. 4. Control solutions in sea state 3, in terms of velocity, control input and electrical power, obtained with the spectral method for $\mu = 1$ (dotted green), and for $\mu = 0.7$ with the spectral (green) and MPC (orange) methods. Also shown on the first graph, the wave excitation torque (dotted blue).

5.3 Sensitivity analysis of MPC performance

In order to understand, and reduce further the differences observed between MPC results and optimal spectral control, a sensitivity analysis on the prediction horizon is carried out, using $N_p = 17, 25, 37, 49$. Furthermore, perfect excitation estimation and prediction are assumed, so as to isolate better the different factors influencing MPC performance.

In theory, under such conditions, increasing the prediction horizon should necessarily improve MPC performance since, for larger N_p, the optimiser has more degrees of freedom to improve the same objective function. However, in practice, the objective function of the offline weighting optimisation problem may have a complicated, non-convex surface. Therefore, it is difficult to ensure that the NMS optimiser converges to the true optimal weightings. In order to investigate how the specific challenges of the offline optimisation might impact MPC performance, three different NMS initialisation methods (abbreviated as M1, M2, M3) are considered:

- In M1, weightings are initialized with a vector of ones. This method was applied during the WECCCOMP.
- In M2, weightings are initialized with independent random values following a uniform distribution within a limited range (0 to 4 in this work).
- In M3, weightings are initialized using the optimal weightings, determined for a smaller value of N_p, padded with zeros for the remaining time steps. This approach ensures that, when increasing N_p, the NMS optimiser always finds a solution with better performance.

Figs. 5 and 6 show the results, in terms of electric power, of the NMS optimisation on the first realisations of SS1 and SS3, with initialisation methods M1-3, and different N_p values. All results are normalised by spectral optimal control values for R1, reported in Table 1.

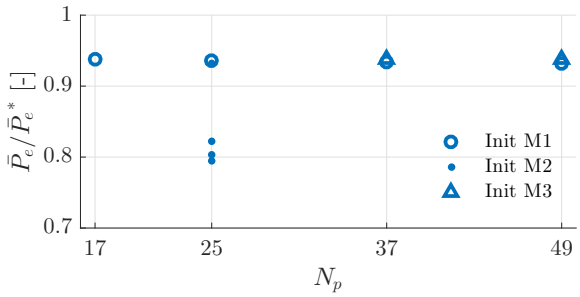

Fig. 5. Optimisation results in SS1 with different prediction horizons and initialisation methods

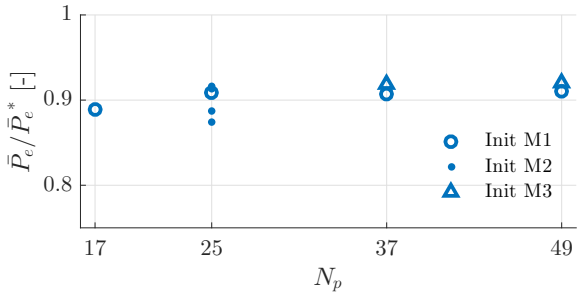

Fig. 6. Optimisation results in SS3 with different prediction horizons and initialisation methods

With M1, in the two sea states, MPC performance improves when increasing N_p from 17 (0.85 s) to 25 (1.25 s) but, unexpectedly, plateaus or even degrades when N_p increases further to 37 and 49. Since, in this scenario, wave estimations and predictions are perfect, such results cannot be accounted for by the increase of prediction errors with the time horizon, but should rather be attributed to the behavior of the NMS optimiser, with the optimisation problem considered and those initial values.

In order to clearly evidence the results sensitivity to the choice of weighting initialisation, the optimisation is run starting from randomly-chosen coefficients, following M2, with $N_p = 25$. As can be appreciated in Figs. 5 and 6, various initialisation possibilities yield diverse performance values, with a particularly large spread of results in SS1. However, very few of the random initial values tested enable the optimiser to find better solutions than starting from M1. Furthermore, weightings determined starting from differing initial values, but having similar performance, may have completely different values, as illustrated in Fig. 7.

Finally, using M3 should ensure that increasing N_p yields better performance. More specifically, weightings optimised with M1 and $N_p = 25$ are used to initialise the optimisation for $N_p = 37$; the resulting weightings are, in turn, employed to initialise the optimisation for $N_p = 49$. However, even with $N_p = 49$ (i.e. twice the "baseline" $N_p = 25$), the difference between MPC and optimal control results only decreases by 1.2% of $\bar{P}_e^*$ for SS3 while, for SS1, there is no significant improvement. While it could be expected that increasing the prediction horizon would bridge the gap between MPC and optimal control results,

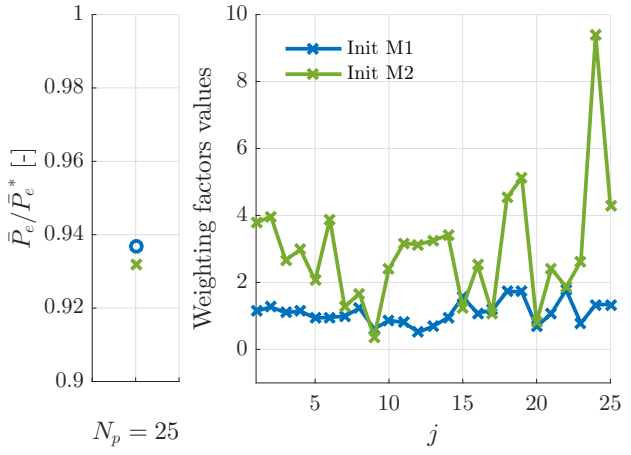

Fig. 7. Optimised weighting values for initialisation methods M1 and M2 in SS1

it doesn't seem to be the case in practice. Furthermore, the offline optimisation time (for NMS to converge) dramatically increases with the control horizon: With $N_p = 49$, the NMS convergence time is almost three times that associated with $N_p = 25$.

6. CONCLUSION

Overall, this study demonstrates that the MPC scheme, proposed by IFPEN for the WECCCOMP, is capable of approaching optimal control results, in terms of electric power (MPC results are only sub-optimal by 8 to 11% in the two sea states considered), trajectory and control input, which is a remarkable achievement, given the relatively short prediction horizon, the errors necessarily associated with wave predictions, and the fact that the real-time control solution relies on a quadratic approximation of the true objective function.

It is interesting to explore how this relatively minor difference could be further reduced. Although perfect wave predictions do improve MPC results by 1 or 2%, they are clearly not sufficient to make the proposed methodology reach optimal control performance, even when the prediction horizon is simultaneously increased. The complexity of the offline MPC weighting optimisation problem may be an obstacle, which prevents longer prediction horizons from improving control results significantly. Therefore, employing another gradient-free search algorithm, such as genetic optimisation, could be investigated in future work to replace the NMS method.

However, it may also well be the case that most of the observed difference, with respect to optimal control results, is inherent to the proposed method, whereby the (non-ideal) efficiency function is approximated by means of fixed coefficients, which can only take the non-ideal efficiency function into account *on average* for a given sea state.

In retrospect, amongst the possibilities considered here, the MPC initialisation method and algorithm setup employed for the WECCCOMP, which had been essentially chosen based on common sense, experience and trial and error, indeed seem to have been an appropriate choice.

In future work, the WECCCOMP wave tank experimental results could also be assessed in the light of spectral optimal control solutions, although it may be difficult to discriminate between the influence of modelling errors and that of control algorithms.

REFERENCES

Faedo, N., Olaya, S., and Ringwood, J.V. (2017). Optimal control, MPC and MPC-like algorithms for wave energy systems: An overview. *IFAC Journal of Systems and Control*, 1, 37–56.

Mérigaud, A. and Ringwood, J.V. (2017). Improving the computational performance of nonlinear pseudospectral control of wave energy converters. *IEEE Transactions on Sustainable Energy*, 9(3), 1419–1426.

Nguyen, H.N., Sabiron, G., Tona, P., Kramer, M.M., and Vidal Sanchez, E. (2016). Experimental validation of a nonlinear MPC strategy for a wave energy converter prototype. In *Proceedings of the 35th International Conference on Ocean, Offshore & Arctic Engineering (OMAE 2016),*. American Society of Mechanical Engineers Digital Collection.

Nguyen, H.N. and Tona, P. (2018). Short-term wave force prediction for wave energy converter control. *Control Engineering Practice*, 75, 26 – 37.

Ogilvie, T. (1964). Recent progress toward the understanding and prediction of ship motions. In *Sixth Symposium on Naval Hydrodynamics*.

Ringwood, J.V., Bacelli, G., and Fusco, F. (2014). Energy-maximizing control of wave-energy converters: The development of control system technology to optimize their operation. *IEEE control systems magazine*, 34(5), 30–55.

Ringwood, J.V., Ferri, F., Ruehl, K., Yu, Y.H., Coe, R.G., Bacelli, G., Weber, J., and Kramer, M.M. (2017). A competition for WEC control systems. In *12th European Wave and Tidal Energy ConferencEuropean Wave and Tidal Energy Conference*.

Tona, P., Sabiron, G., Mérigaud, A., Nguyen, H.N., and Ngo, C. (2020). Experimental assessment of the IFPEN solution to the WEC Control Competition. In *Proc. Of OMAE 2020, OMAE2020-18669, Fort Lauderdale, US*.

Tona, P., Sabiron, G., and Nguyen, H.N. (2019). An energy-maximising MPC solution to the WEC Control Competition. In *Proceedings of the 38th International Conference on Ocean, Offshore & Arctic Engineering (OMAE 2019)*. American Society of Mechanical Engineers Digital Collection.